Effects of sea surface temperature, cloud radiative and microphysical processes, and diurnal variations on rainfall in equilibrium cloud-resolving model simulations*

Jiang Zhe(蒋 哲)[a], Li Xiao-Fan(李小凡)[b], Zhou Yu-Shu(周玉淑)[c], and Gao Shou-Ting(高守亭)[c]†

[a] *Institute of Remoting Sensing Applications, Chinese Academy of Sciences, Beijing* 100101, *China*

[b] *NOAA/NESDIS/Center for Satellite Applications and Research Camp Springs, Maryland* 21029, *USA*

[c] *Laboratory of Cloud-Precipitation Physics and Severe Storms (LACS), Institute of Atmospheric Physics, Chinese Academy of Sciences, Beijing* 100029, *China*

(Received 9 October 2011; revised manuscript received 12 January 2012)

The effects of sea surface temperature (SST), cloud radiative and microphysical processes, and diurnal variations on rainfall statistics are documented with grid data from the two-dimensional equilibrium cloud-resolving model simulations. For a rain rate of higher than 3 mm·h^{-1}, water vapor convergence prevails. The rainfall amount decreases with the decrease of SST from 29 °C to 27 °C, the inclusion of diurnal variation of SST, or the exclusion of microphysical effects of ice clouds and radiative effects of water clouds, which are primarily associated with the decreases in water vapor convergence. However, the amount of rainfall increases with the increase of SST from 29 °C to 31 °C, the exclusion of diurnal variation of solar zenith angle, and the exclusion of the radiative effects of ice clouds, which are primarily related to increases in water vapor convergence. For a rain rate of less than 3 mm·h^{-1}, water vapor divergence prevails. Unlike rainfall statistics for rain rates of higher than 3 mm·h^{-1}, the decrease of SST from 29 °C to 27 °C and the exclusion of radiative effects of water clouds in the presence of radiative effects of ice clouds increase the rainfall amount, which corresponds to the suppression in water vapor divergence. The exclusion of microphysical effects of ice clouds decreases the amount of rainfall, which corresponds to the enhancement in water vapor divergence. The amount of rainfall is less sensitive to the increase of SST from 29 °C to 31 °C and to the radiative effects of water clouds in the absence of the radiative effects of ice clouds.

Keywords: rain rate, sea surface temperature, radiative and microphysical effects of ice and water clouds, diurnal variation

PACS: 42.68.Ge, 92.60.N–, 92.60.jf, 92.60.Wc **DOI:** 10.1088/1674-1056/21/5/054215

1. Introduction

Precipitation is a result of the strong development of convective systems associated with the release of unstable energy. Precipitation comes directly from cloud microphysical processes as a result of convective development, which is affected by environmental thermodynamic conditions such as sea surface temperature (SST) and diurnal variation of solar zenith angle.[1−11] Cui and Li[12] analyzed the surface rainfall budgets proposed by Gao *et al.*[13] over rainfall and rainfall-free regions and found that the enhancement of surface evaporation by the increase in SST over rainfall-free regions supports the transport of water vapor from rainfall-free regions into rainfall regions. Ping *et al.*[14] revealed that the exclusion of the radiative effects of ice clouds enhances rainfall by increasing the surface evaporation flux whereas the exclusion of ice microphysical effects reduces the amount of rainfall by suppressing the surface evaporation flux. Zhou and Li[15] showed that the increase in surface evaporation flux over rainfall-free regions caused by an increase in SST from 29 °C to 31 °C leads to an increase in the water vapor transport to rainfall regions. Previous rainfall studies mainly focus on convective and stratiform regions, which are from grids where the rain rate is associated with different rainfall processes. The analysis of rainfall statistics from an accumulation of each grid

*Project supported by the National Basic Research Program of China (Grant No. 2012CB417201) and the National Natural Science Foundation of China (Grant Nos. 41075034, 40930950, 40975034, and 41075044).

†Corresponding author. E-mail: gst@mail.iap.ac.cn

© 2012 Chinese Physical Society and IOP Publishing Ltd

will enhance the understanding of rainfall processes and their responses to changes of environmental conditions and cloud-radiation interaction processes. Thus, the effects of SST, cloud radiative and microphysical processes, and diurnal variations on rainfall statistics are documented in this study through the analysis of grid-scale data from a series of two-dimensional equilibrium cloud-resolving model simulations. Precipitation intensity, which is denoted by the surface rain rate, will be analyzed, in this study. The questions asked in this study are: how different are the rainfall processes between weak and strong precipitation? What are the responses of cumulative rainfall from each grid to SST, cloud radiative and microphysical processes, and diurnal variations? How do these factors and processes impact rainfall statistics? The rest of the paper is organized as follows: in Section 2, the model and the experiments will be briefly described. The results are presented in Section 3. A summary is given in Section 4.

2. Model and experiments

The data analyzed in this study are from an equilibrium cloud-resolving model simulation conducted by Gao *et al.*[16,17] The cloud-resolving model used in these equilibrium model simulations is a two-dimensional version of the model used by Sui *et al.*[18,19] and further modified by Li *et al.*[20] The model was originally developed by Soong and Ogura,[21] Soong and Tao,[22] and Tao and Simpson.[23] The model has cyclic lateral boundaries and includes prognostic equations for the mixing ratios of cloud species (cloud water, raindrops, cloud ice, snow, and graupel), and prognostic equations for potential temperature, specific humidity, and perturbation momentum. The model also has cloud microphysical parameterization schemes,[24−28] and solar and thermal infrared radiation parameterization schemes.[29,30] The model uses a horizontal domain of 768 km, a horizontal grid resolution of 1.5 km, 33 vertical levels, and a time step of 12 s. Detailed model descriptions can be found in Gao and Li.[31]

All equilibrium model simulations are integrated for 40 days with the model imposed with a time- and height-invariant large-scale zonal wind of -4 m·s^{-1} and zero large-scale vertical velocity. The vertical profiles of temperature and specific humidity observed at 156°E and 1.75°S during the Tropical Ocean Global Atmosphere Coupled Ocean Atmosphere Response Experiment at 0400 LST 19 December 1992[32] are used as the initial conditions. The increase in SST increases the mass-weighted mean air temperature and precipitable water whereas the diurnal variations of SST cause cooling.[16] The diurnal variation of solar zenith angle produces atmospheric warming and moistening. The exclusion of radiative and microphysical effects of ice clouds[14] and cloud radiative effects[17] generates atmospheric cooling and drying.

The simulations are summarized in Table 1. Experiments SST29, SST31 and SST27 use the same model setup except that different time-invariant SSTs of 29, 31 and 27 °C are used, respectively. These experiments are used to study the effects of SST. Experiment SST29M has a time-invariant solar zenith angle whereas SST29 has a diurnally varied solar zenith angle. The comparison between SST29 and SST29M shows the effects of diurnally varied solar radiative heating. Experiments SST29D1 and SST29D2 have diurnally varied SSTs with a mean of 29 °C and diurnal differences (maximum SST minus minimum SST) of 1 and 2 °C, respectively. The comparison of SST29D1 and SST29D2 with SST29 shows the effects of diurnal variation of SSTs. Experiments SST29NIR and SST29NWR are identical to SST29 except that SST29NIR and SST29NWR exclude the radiative effects of ice and water clouds, respectively, by setting the mixing ratios of ice and water hydrometeors to be zero in the calculations of optical depth and radiation. The comparison between SST29NIR and SST29 shows the radiative effects of ice clouds, whereas the comparison between SST29NWR and SST29 reveals the radiative effects of water clouds when the radiative effects of ice clouds are turned on. Experiment SST29NCR is identical to SST29NIR except that SST29NCR excludes the radiative effects of water clouds by setting the mixing ratios of water hydrometeors (cloud water and raindrops) to be zero in the calculations of optical depth and radiation. The comparison between SST29NCR and SST29NIR reveals the radiative effects of water clouds when the radiative effects of ice clouds are turned off. Experiment SST29NIM excludes ice–cloud variables and the associated ice microphysical and radiative processes by turning off the ice microphysics scheme during the model integration. The comparison between SST29NIM and SST29NIR shows the microphysical effects of ice clouds when the radiative effects of ice clouds are excluded. The rainfall statistics are documented using the grid data from equilibrium model simulations over 10 days.

Table 1. Summary of the equilibrium experiments.

Experiment	SST	Solar zenith angle	Radiation	Ice microphysics
SST29	time-invariant (29 °C)	diurnally-varied	yes	yes
SST27	time-invariant (27 °C)	diurnally-varied	yes	yes
SST31	time-invariant (31 °C)	diurnally-varied	yes	yes
SST29D1	diurnally-varied with mean of 29 °C and maximum diurnal difference of 1 °C	diurnally varied	yes	yes
SST29D2	diurnally-varied with mean of 29 °C and maximum diurnal difference of 2 °C	diurnally varied	yes	yes
SST29M	time-invariant (29 °C)	time-invariant	yes	yes
SST29NCR	time-invariant (29 °C)	diurnally-varied	no for both water and ice clouds	yes
SST29NIR	time-invariant (29 °C)	diurnally varied	no for ice clouds	yes
SST29NWR	time-invariant (29 °C)	diurnally-varied	no for water clouds	yes
SST29NIM	time-invariant (29 °C)	diurnally-varied	no for ice clouds	no

To examine the roles of water vapor and clouds in surface rainfall processes, the surface rainfall equation was derived by combining water vapor and cloud equations.[13] The surface rain rate ($P_{\rm S}$) can be written as

$$P_{\rm S} = Q_{\rm WVT} + Q_{\rm WVF} + Q_{\rm WVE} + Q_{\rm CM}, \tag{1}$$

where

$$Q_{\rm WVT} = -\frac{\partial[q_{\rm v}]}{\partial t}, \tag{1a}$$

$$Q_{\rm WVF} = -\Big[\bar{u}^{\rm o}\frac{\partial \bar{q}_{\rm v}^{\rm o}}{\partial x}\Big] - \Big[\bar{w}^{\rm o}\frac{\partial \bar{q}_{\rm v}}{\partial z}\Big] - \Big[\bar{w}^{\rm o}\frac{\partial q'_{\rm v}}{\partial z}\Big] - \Big[w'\frac{\partial \bar{q}_{\rm v}}{\partial z}\Big] - \Big[\frac{\partial}{\partial x}(\bar{u}^{\rm o}+u')q'_{\rm v}\Big], \tag{1b}$$

$$Q_{\rm WVE} = E_{\rm s}, \tag{1c}$$

$$Q_{\rm CM} = -\frac{\partial[q_5]}{\partial t} - \Big[\frac{\partial}{\partial x}(\bar{u}^{\rm o}q_5)\Big] - \Big[\frac{\partial}{\partial x}(u'q_5)\Big]. \tag{1d}$$

Here, $q_{\rm v}$ is the specific humidity; u and w are the zonal and vertical components of wind, respectively; $E_{\rm s}$ is the surface evaporation rate; $q_5 = q_{\rm c}+q_{\rm r}+q_{\rm i}+q_{\rm s}+q_{\rm g}$, $q_{\rm c}, q_{\rm r}, q_{\rm i}, q_{\rm s}, q_{\rm g}$ are the mixing ratios of cloud water, raindrops, cloud ice, snow, and graupel, respectively; overbar denotes a spatial mean; prime is a perturbation from spatial mean; $[()] = \int_{z_{\rm b}}^{z_{\rm t}} \bar{\rho}()\,{\rm d}z$, with $z_{\rm t}$ and $z_{\rm b}$ being the heights of the top and bottom of the model atmosphere respectively; and superscript $^{\rm o}$ is an imposed COARE - observed value. Equation (1) states that the surface rain rate is contributed by local vapor change ($Q_{\rm WVT}$), vapor convergence ($Q_{\rm WVF}$), surface evaporation ($Q_{\rm WVE}$), and cloud source/sink ($Q_{\rm CM}$). Positive values of $Q_{\rm WVT}$, $Q_{\rm WVF}$, and $Q_{\rm CM}$ denote local atmospheric drying, water vapor convergence, and local hydrometeor loss/ hydrometeor convergence, respectively; whereas negative $Q_{\rm WVT}$, $Q_{\rm WVF}$, and $Q_{\rm CM}$ denote local atmospheric moistening, water vapor divergence, and local hydrometeor gain/hydrometeor divergence, respectively.

The comparison studies between two-dimensional (2D) and three-dimensional (3D) model simulations show some differences. Moncrieff and Miller[33] revealed that the 3D cross-over flow patterns of tropical squall lines can only be simulated in the 3D model framework. Rotunno *et al.*[34] found that the basic dynamics associated with long-lived squall lines in a strong low-level shear can be reasonably simulated in a 2D model framework. Xu *et al.*[35], Gao *et al.*,[36] and Gao[37] found differences between 2D and 3D dynamics. The 2D and 3D model simulations reveal a lot of similarities in terms of collective thermodynamic feedback effects, vertical transport of mass, sensible heat, and moisture, thermodynamic fields, surface heat fluxes, surface precipitation, precipitation efficiency, and vorticity vectors.[38−45] Thus, 2D model simulations can be used to explore the effects of SST, cloud radiation and microphysical processes, and diurnal variations on rainfall statistics in this study.

3. Results

The amount of cumulative surface rainfall is calculated by accumulating surface rainfall at each bin of the surface rain rate every 3 mm·h^{-1} (e.g., 0–3 mm·h^{-1}, 3–6 mm·h^{-1}). Similar calculations are also applied to data of $Q_{\rm WVT}$, $Q_{\rm WVF}$, $Q_{\rm WVE}$, and $Q_{\rm CM}$ to obtain cumulative $Q_{\rm WVT}$, $Q_{\rm WVF}$, $Q_{\rm WVE}$, and $Q_{\rm CM}$ amount. In the control experiment SST29, the amount of cumulative surface rainfall generally decreases as the surface rain rate increases (Fig. 1(a)).

The amount of cumulative rainfall is mainly attributed to water vapor convergence, except for the surface rain rate of 3 mm·h^{-1} where water vapor divergence occurs (Fig. 1(c)) and an amount of cumulative rainfall is from surface evaporation (Fig. 1(d)), hydrometeor convergence/local hydrometeor loss (Fig. 1(e)), and local atmospheric drying (Fig. 1(b)). The decrease of cumulative rainfall for the surface rain rate of 3–21 mm·h^{-1} is significantly larger than that for a surface rain rate of 21–39 mm·h^{-1}. The amount of cumulative rainfall is small for strong surface rain rates of higher than 39 mm·h^{-1}. The amounts of cumulative rainfall for surface rain rates of 0–3 mm·h^{-1}, 3–21 mm·h^{-1}, 21–39 mm·h^{-1} and higher than 39 mm·h^{-1}, are 12.5%, 55.1%, 22.7%, and 9.7% of the total cumulative rainfall amount respectively. Thus, effects of SST, cloud radiation and microphysical processes, and diurnal variations on rainfall statistics will be separately examined with surface rain rates lower than 3 mm·h^{-1}, 3–21 mm·h^{-1}, 21–39 mm·h^{-1}, and higher than 3 mm·h^{-1}.

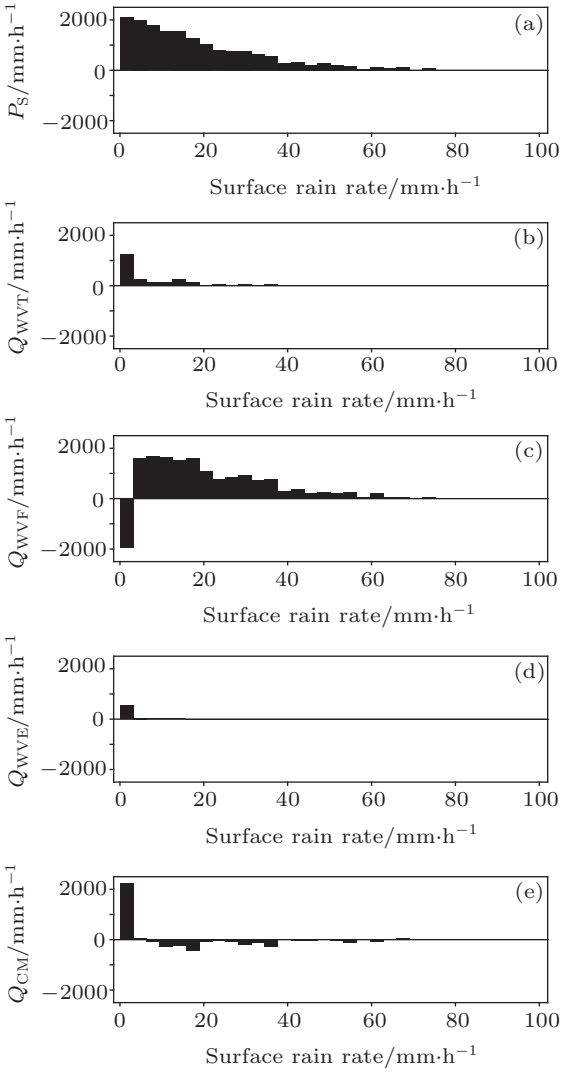


Fig. 1. Amount of cumulative surface rainfall (P_S) and contributions from minus local vapor storage (Q_{WVT}), water vapor convergence (Q_{WVF}), surface evaporation (Q_{WVE}), and hydrometeor convergence minus storage (Q_{CM}) as a function of surface rain rate (mm·h^{-1}) in SST29.

3.1. Rainfall statistics for a surface rain rate of lower than 3 mm·h^{-1}

The cumulative rainfall amounts are 4.4 % larger in SST31 and 20.1% larger in SST27 than in SST29 (Fig. 2(a)). The increase of rainfall in SST27 is associated with the decrease in water vapor divergence, whereas the rainfall increase in SST31 is primarily related to the increase in local atmospheric drying. The inclusion of diurnal variations of SST decreases the amount of rainfall by 3.0% in SST29D1 (Fig. 2(a)) and 12.0% in SST29D2 (Fig. 2(b)). The rainfall decreases correspond primarily to the increase in water vapor divergence. The exclusion of solar zenith angle in SST29M increases the amount of rainfall by 16.0%, which is primarily associated with the increase in local atmospheric drying (Fig. 2(b)).

The decrease in the amount of rainfall caused by the exclusion of microphysical effects of ice clouds (14.2%) is twice as large as that by the exclusion of radiative effects of ice clouds (6.8%) (Figs. 2(b) and 2(c)). The decrease in the amount of rainfall caused by the exclusion of microphysical effects of ice clouds is from the increase in local hydrometeor gain/hydrometeor divergence, the decrease in surface evaporation, and local atmospheric change from drying in SST29NIR to moistening in SST29NIM, which is largely offset by the increase in water vapor convergence. The decrease in the amount of rainfall caused by the exclusion of radiative effects of ice clouds is from the decrease in water vapor convergence. The rainfall amount is less sensitive to radiative effects of water clouds when radiative effects of ice clouds are absent because the increase in water vapor convergence is nearly balanced by the decrease in local atmospheric drying (Fig. 2(c)). When radiative effects of ice clouds are present, the exclusion of radiative effects of water clouds increases the rainfall amount by 6.7% in SST29NWR (Fig. 2(c)), which is primarily associated with the increase in water vapor convergence (Fig. 2(c)).

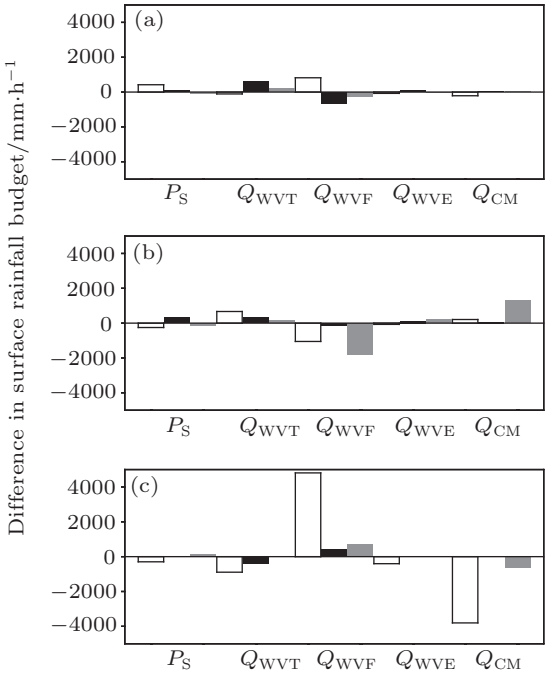


Fig. 2. Difference in cumulative surface rainfall (P_S) and contributions from minus local vapor storage (Q_{WVT}), water vapor convergence (Q_{WVF}), surface evaporation (Q_{WVE}), and hydrometeor convergence minus storage (Q_{CM}) for surface rain rate of 0–3 mm·h^{-1} for (a) SST27-SST29 (open bar), SST31-SST29 (black bar), SST29D1-SST29 (grey bar), (b) SSTD2-SST29 (open bar), SST29M-SST29 (black bar), SST29NIR-SST29 (grey bar), and (c) SST29NIM-SST29NIR (open bar), SST29NCR-SST29NIR (black bar), SST29NWR-SST29 (grey bar).

3.2. Rainfall statistics for a surface rain rate of 3–21 mm·h^{-1}

The change of SST causes the decrease of cumulative rainfall regardless of whether SST increases or decreases (Fig. 3(a)). The cumulative rainfall amounts are 10.3% smaller in SST27 and 7.3% smaller in SST31 than that in SST29. The decrease of rainfall amount from SST29 to SST31 is associated with the increase in local hydrometeor gain/hydrometeor divergence. The 59.1% decrease in rainfall amount from SST29 to SST27 is from the increase of local hydrometeor concentration/hydrometeor divergence and the 37.3% decrease is from the decreases in local atmospheric drying and water vapor convergence.

The inclusion of diurnal variation of SST decreases rainfall by 8.7% in SST29D1 (Fig. 3(a)) and 13.1% in SST29D2 (Fig. 3(b)). The amplification of diurnal variation of SST accelerates the decrease of rainfall. The decreases of rainfall amount are associated with the decreases in water vapor convergence and the increase in local hydrometeor gain/hydrometeor divergence when the diurnal variations of SST are included in the two experiments. The decrease in water vapor convergence and the increase in local hydrometeor gain /hydrometeor divergence are primarily responsible for the decreases of rainfall amount in SST29D1 and SST29D2, respectively. The exclusion of diurnal variation of solar zenith angle in SST29M increases rainfall amount by 3.3%, which corresponds to the increases in local atmospheric drying and water vapor convergence (Fig. 3(b)).

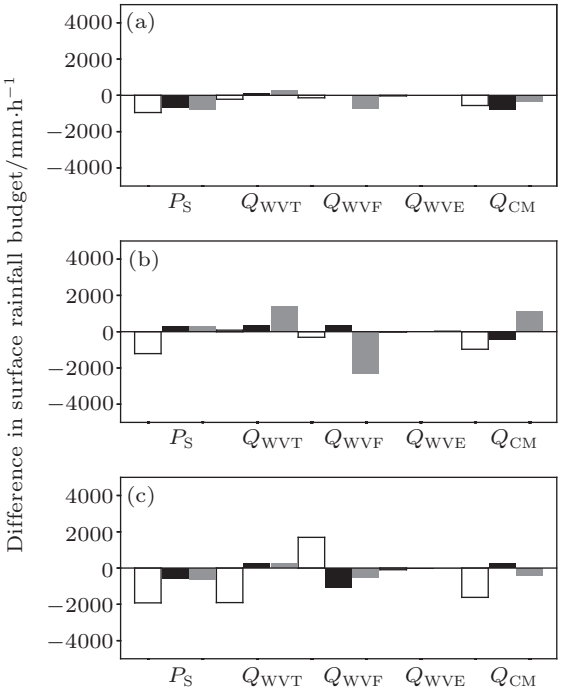


Fig. 3. Same as in Fig. 2, except for surface rain rate of 3–21 mm·h^{-1}.

The exclusion of radiative effects of ice clouds increases rainfall in SST29NIR by 3.5% (Fig. 3(b)), whereas the exclusion of microphysical effects of ice clouds decreases rainfall amount in SST29NIM by 20.2% (Fig. 3(c)). The increase in rainfall for SST29NIR-SST29 is associated with the increase in local atmospheric drying and local hydrometeor gain/hydrometeor divergence in SST29 and local hydrometeor loss/hydrometeor convergence in SST29NIR, while the exclusion of radiative effects of ice clouds decreases water vapor convergence by 25.2%. The large decrease in rainfall for SST29NIM-SST29NIR is related to the dramatic decrease in local atmospheric drying and large local atmospheric gain/hydrometeor divergence in SST29NIM.

The exclusion of radiative effects of water clouds similarly decreases the amount of rainfall, which is insensitive to radiative effects of ice clouds (Fig. 3(c)). The decrease in rainfall for SST29NIM-SST29NIR corresponds mainly to the decrease in water vapor convergence by the exclusion of radiative effects of water clouds when radiative effects of ice clouds are turned off in the two experiments. The decrease in rainfall for SST29NWR-SST29 is from the decrease in water vapor convergence and increase in local hydrometeor gain/hydrometeor divergence.

3.3. Rainfall statistics for surface rain rate of 21–39 mm·h^{-1}

The 2 °C decrease of SST decreases the amount of rainfall by 36.9% whereas the 2 °C increase of SST increases rainfall by 32.2% (Fig. 4(a)). The decrease and increase of rainfall are, respectively, associated with the decrease and increase in water vapor convergence in SST27 and SST31. Cumulative rainfall amounts are less sensitive to diurnal variations of SST (Figs. 4(a) and 4(b)). These are due to the fact that the increase in water vapor convergence is nearly offset by the increase in local hydrometeor gain/hydrometeor divergence. The exclusion of solar zenith angle in SST29M leads to the 19.1 % increase of rainfall, which primarily corresponds to the increase in water vapor convergence (Fig. 4(b)).

The exclusion of radiative effects of ice clouds increases the amount of rainfall by 42.1% (Fig. 4(b)), whereas the exclusion of microphysical effects of ice clouds decreases rainfall by 43.8% (Fig. 4(c)). The rainfall increase for SST29NIR-SST29 and rainfall decrease for SST29NIM-SST29NIR are, respectively, associated with the increase and decrease in water vapor convergence. The exclusion of radiative effects of water clouds decreases rainfall amount by 8.6% when radiative effects of ice clouds are turned off, whereas it increases rainfall by 4.1% when radiative effects of ice clouds are turned on (Fig. 4(c)). The rainfall decrease for SST29NCR-SST29NIR is associated with the decrease in water vapor convergence. The small rainfall amount increase for SST29NWR-SST29 is related to the enhancement of local atmospheric drying while the decrease in water vapor convergence is nearly cancelled by the decrease in local hydrometeor gain/hydrometeor divergence.

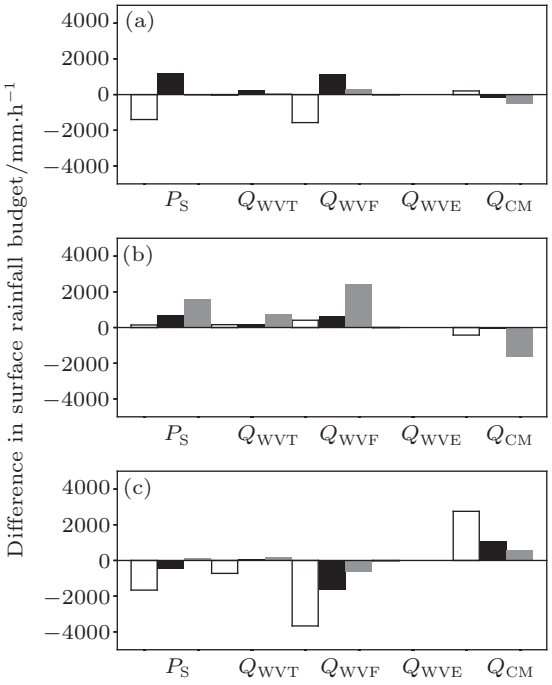


Fig. 4. Same as in Fig. 2, except for surface rain rate of 21–39 mm·h^{-1}.

3.4. Rainfall statistics for a surface rain rate higher than 39 mm·h^{-1}

The 61.7% decrease of rainfall by the decrease of SST from 29 °C to 27 °C is associated with the decrease in water vapor convergence, whereas the 48.3% increase of rainfall amount by the increase of SST from 29 °C to 31 °C is primarily related to the increase in water vapor convergence (Fig. 5(a)). The inclusion of diurnal variation of SST in SST29D1 increases the rainfall amount by 19.8%, which primarily corresponds to the increase in water vapor convergence (Fig. 5(a)). The increase of diurnal difference of SST from 1 °C in SST29D1 to 2 °C in SST29D2 leads to the 7.5% decrease of rainfall amount, which corresponds to the decrease in water vapor convergence (Fig. 5(b)). The exclusion of diurnal variation of solar zenith angle in SST29M increases rainfall amount by 6.3% due to the decrease in local hydrometeor gain/hydrometeor divergence (Fig. 5(b)).

The exclusion of radiative effects of ice clouds increases the amount of rainfall by 80.8%, which corresponds primarily to the increase in water vapor convergence (Fig. 5(b)). The exclusion of microphysical effects of ice clouds decreases rainfall by 89.9%, which is primarily from the decrease in water vapor convergence (Fig. 5(c)). The exclusion of radiative effects of water clouds increases rainfall amount by 20.4% when

radiative effects of ice clouds are turned off, whereas it decreases rainfall amount by 10.5% when radiative effects of ice clouds are turned on (Fig. 5(c)). The increase and decrease of rainfall amount are, respectively, associated with the increase in water vapor convergence in SST29NCR and the decrease in water vapor convergence in SST29NWR.

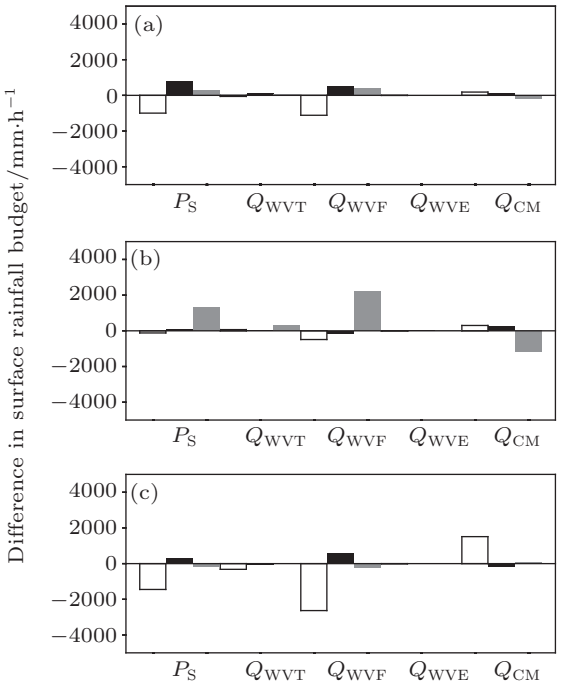


Fig. 5. Same as in Fig. 2, except for surface rain rate of higher than 39 mm·h^{-1}.

4. Summary and discussion

Effects of sea surface temperature (SST), cloud radiative and microphysical processes, and diurnal variations on rainfall statistics are investigated by analyzing two-dimensional equilibrium cloud-resolving model simulation data from Gao *et al.*[16], Ping *et al.*,[14] and Gao.[17] The equilibrium model simulations are conducted using the two-dimensional cloud-resolving model imposed with zero large-scale vertical velocity and a time- and height-invariant large-scale zonal wind. The rainfall statistics are categorized by the rain rate and calculated with grid model simulation data based on surface rainfall budgets that are linked to water vapor and cloud processes. The main results include:

1) In the control experiment, the cumulative rainfall amount for light rain (the rain rate is less than 3 mm·h^{-1}), which is about 12.5% of the total amount of rainfall, is primarily associated with the local hydrometeor loss/hydrometeor convergence and local atmospheric drying while water vapor divergence prevails. The rainfall amount for rain rate of higher than 3 mm·h^{-1} corresponds to water vapor convergence.

2) In general (for rain rate of higher than 3 mm·h^{-1}), the decrease of SST from 29 °C to 27 °C, the inclusion of diurnal variation of SST, and the exclusion of microphysical effects of ice clouds and radiative effects of water clouds decrease rainfall amount primarily through suppressing water vapor convergence. The increase of SST from 29 °C to 31 °C, the exclusion of diurnal variation of solar zenith angle, and the exclusion of radiative effects of ice clouds increase rainfall amount primarily via enhancing water vapor convergence. The water vapor convergence over rainfall regions are balanced by the water vapor divergence over rainfall-free regions due to imposed zero large-scale vertical velocity in the model with cyclic boundaries; the water divergence is largely balanced by surface evaporation over rainfall-free regions.[12] Thus, SST, cloud radiation and microphysical processes, and diurnal variations affect rainfall amount by changing surface evaporation over rainfall-free regions.

3) For light rain, the 2 °C decrease of SST and the exclusion of radiative effects of water clouds with the presence of radiative effects of ice clouds increase rainfall amount, respectively by 20.1% and 6.7% through suppressing water vapor divergence. The exclusion of diurnal variation of solar zenith angle and the 2 °C increase of SST increase rainfall amounts, respectively, by 16.0% and 4.4% via enhancing local atmospheric drying. The inclusion of diurnal variations of SST with diurnal difference of 2 °C and the exclusion of radiative effects of ice clouds decrease rainfall amount, respectively, by 12% and 6.8% through enhancing water vapor divergence. The exclusion of microphysical effects of ice clouds decreases rainfall amount by 14.2% primarily via enhancing local hydrometeor gain/hydrometeor divergence. The rainfall amount is less sensitive to diurnal variations of SST with diurnal difference of 1 °C and radiative effects of water clouds with the absence of radiative effects of ice clouds.

Acknowledgement

The authors thank Dr. W. K. Tao at NASA/GSFC for his cloud-resolving model.

References

[1] Yoshizaki M 1986 *J. Meteor. Soc. Japan* **64** 469

[2] Nicholls M E 1987 *Mon. Wea. Rev.* **115** 3055

[3] McCumber M, Tao W K, Simpson J, Penc R and Soong S T 1991 *J. Appl. Meteor.* **30** 985

[4] Tao W K, Simpson J and Soong S T 1991 *Mon. Wea. Rev.* **119** 2699

[5] Lau K M, Sui C H and Tao W K 1993 *Bull. Amer. Meteor. Soc.* **74** 1313

[6] Lau K M, Sui C H, Chou M D and Tao W K 1994 *Geophys. Res. Lett.* **21** 1157

[7] Wu X and Moncrieff M W 1999 *J. Geophys. Res.* **104** 6093

[8] Wu X 2002 *J. Atmos. Sci.* **59** 1885

[9] Grabowski W W and Moncrieff M W 2001 *Quart. J. Roy. Meteor. Soc.* **127** 445

[10] Grabowski W W 2001 *J. Climate* **13** 2306

[11] Grabowski W W 2003 *Quart. J. Roy. Meteor. Soc.* **129** 67

[12] Cui X and Li X 2006 *J. Geophys. Res.* **111** D17112

[13] Gao S, Cui X, Zhou Y and Li X 2005 *J. Geophys. Res.* **110** D10202

[14] Ping F, Luo Z and Li X 2007 *Mon. Wea. Rev.* **135** 2794

[15] Zhou Y and Li X 2009 *Atmos. Res.* **92** 212

[16] Gao S, Zhou Y and Li X 2007 *J. Atmos. Sci.* **64** 656

[17] Gao S 2008 *J. Geophys. Res.* **113** D03108

[18] Sui C H, Lau K M, Tao W K and Simpson J 1994 *J. Atmos. Sci.* **51** 711

[19] Sui C H, Li X, and Lau K M 1998 *J. Atmos. Sci.* **55** 2345

[20] Li X, Sui C H, Lau K M and Chou M D 1999 *J. Atmos. Sci.* **56** 3028

[21] Soong S T and Ogura Y 1980 *J. Atmos. Sci.* **37** 2035

[22] Soong S T and Tao W K 1980 *J. Atmos. Sci.* **37** 2016

[23] Tao W K and Simpson J 1993 *Terr. Atmos. Oceanic Sci.* **4** 35

[24] Lin Y L, Farley R D and Orville H D 1983 *J. Climate Appl. Meteor.* **22** 1065

[25] Rutledge S A and Hobbs P V 1983 *J. Atmos. Sci.* **40** 1185

[26] Rutledge S A and Hobbs P V 1984 *J. Atmos. Sci.* **41** 2949

[27] Tao W K, Simpson J and McCumber M 1989 *Mon. Wea. Rev.* **117** 231

[28] Krueger S K, Fu Q, Liou K N and Chin H N S 1995 *J. Appl. Meteor.* **34** 281

[29] Chou M D, Kratz D P and Ridgway W 1991 *J. Climate* **4** 424

[30] Chou M D, Suarez M J, Ho C H, Yan M M H and Lee K T 1998 *J. Atmos. Sci.* **55** 201

[31] Gao S and Li X 2008 *Cloud-Resolving Modeling of Convective Processes* (Berlin: Springer) pp. 1–206

[32] Sui C H, Li X, Yang M J and Huang H L 2005 *J. Atmos. Sci.* **62** 4358

[33] Moncrieff M W and Miller M J 1976 *Quart. J. Roy. Meteor. Soc.* **102** 373

[34] Rotunno R, Klemp J B and Weisman M L 1988 *J. Atmos. Sci.* **45** 463

[35] Xu K M, Cederwall R T, Donner L J, Grabowski W W, Guichard F, Johnson D E, Khairoutdinov M, Krueger S K, Petch J C, Randall D A, Seman C J, Tao W K, Wang D, Xie S C, Yio J J and Zhang M H 2002 *Quart. J. Roy. Meteor. Soc.* **128** 593

[36] Gao S, Cui X, Zhou Y, Li X and Tao W K 2005 *J. Geophys. Res.* **110** D17104

[37] Gao S 2007 *J. Geophys. Res.* **112** D18109

[38] Tao W K and Soong S T 1986 *J. Atmos. Sci.* **43** 2653

[39] Tao W K, Simpson J and Soong S T 1987 *J. Atmos. Sci.* **44** 3175

[40] Grabowski W W, Wu X, Moncrieff M W and Hall W D 1998 *J. Atmos. Sci.* **55** 3264

[41] Tompkins A M 2000 *Mon. Wea. Rev.* **128** 1521

[42] Khairoutdinov M F and Randall D A 2003 *J. Atmos. Sci.* **60** 607

[43] Gao S, Ping F, Li X and Tao W K 2004 *J. Geophys. Res.* **109** D14106

[44] Gao S, Li X, Tao WK, Shie C L and Lang S 2007 *J. Geophys. Res.* **112** D01105

[45] Sui C H, Lau K M, Takayabu Y N and Short D 1997 *J. Atmos. Sci.* **54** 639